

Dynamic Analysis of Evaporator Characteristics

Jae-Dol Kim*, Jung-In Yoon* and Hag-Geun Ku**

(Received August 6, 1996)

An analysis of the dynamic characteristics in an evaporator was numerically performed for control and design of the refrigeration and air conditioning systems. The important factors, such as refrigerant flow rate, inlet enthalpy, inlet air velocity and air temperature, are incorporated with this analysis. An evaporator is modeled for the dynamic characteristics analysis separated into three regions which are the two-phase region, the saturated vapor region and the superheated vapor region. The basic equations of each region were derived in the continuity, heat energy equilibrium and heat transfer equations. The transfer functions of the dynamic characteristics were obtained by the linearization and Laplace transformation. The dynamic response characteristics were evaluated on the Bode diagram with the frequency response method. These results may be used for the analysis of the dynamic characteristics and design in the total system.

Key Words : Dynamic Characteristics, Refrigeration and Air Conditioning Systems, Transfer Functions, Frequency Response, Evaporator

Nomenclature

| | |
|--|---|
| <p>A : Area, (m²)</p> <p>C_m : Heat capacity, (J/kg · K)</p> <p>H : Enthalpy, (J/kg)</p> <p>i : Dimensionless length, (-)</p> <p>L : Tube length, (m)</p> <p>M : Mass flow rate, (kg/s)</p> <p>Q : Heat transfer capacity, (W)</p> <p>t : Time, (sec)</p> <p>X_D : Open area of the expansion valve, (-)</p> <p>α : Heat transfer coefficient, (W/m² · K)</p> <p>θ : Temperature, (K)</p> <p>ρ : Density, (kg/m³)</p> | <p>4 : Average of boundary 3~5</p> <p>a : Air or air side</p> <p>d : Discharge</p> <p>g : Saturated vapor</p> <p>i : Inside circumference</p> <p>in : Inlet</p> <p>m : Tube wall</p> <p>o : External circular</p> <p>out : Outlet</p> <p>r : Refrigerant</p> <p>out : Outlet</p> <p>s : Superheated vapor</p> <p>shm : Average value of internal division</p> |
|--|---|

Subscripts

| | |
|-----|------------------------------|
| — | : Average values of integral |
| * | : Dimensionless |
| 0 | : Steady state |
| 1~6 | : Each boundary |
| 2 | : Average of boundary 1~3 |

* Dept. of Refrigeration and Air Conditioning Engineering, Pukyong National University

** Dept. of Gas and Refrigeration, Dong Myung College

1. Introduction

Recently high efficiency and comfort under wide scope of conditions have been required for the design of the refrigeration and air conditioning systems. However, the optimal control and sufficient cycle efficiencies are not obtained easily in the total operating scope. That is the reason why the dynamic characteristics analysis of the

refrigeration and air conditioning systems is very significant. Each component of the dynamic characteristics such as the compressor, the condenser, evaporator and expansion valve, etc., is necessary to be taken into account in order to analyze the dynamic characteristics of the refrigeration and air conditioning systems, and an analysis of the total dynamic characteristics that combines each component is also required (Higuchi, 1986; Higuchi, 1987; Matsuoka, 1988; Kim, et al., 1994; Kim, et al., 1996).

Since most refrigeration and air conditioning systems operate under various conditions, pure steady state does not exist. Especially if the capacity controllers are fitted to a system, investigations should not only be limited to the steady state analysis but should also include the unsteady state or dynamic analysis (Hiromu, 1985; Honma, 1992; Yasuda, et al., 1992; Wang, et al., 1991; Tanaka, et al., 1980). Though only a few experimental and theoretical studies have been done until now, the analysis of this part has not offered any clear answer. Therefore, further analysis of the dynamic characteristics in an evaporator is essential to analyze the refrigeration and air conditioning system precisely. Accordingly, the object of this study is to give an analysis of the dynamic characteristics of the evaporator in order

to analyze the dynamic characteristics of the total refrigeration and air conditioning system. As the results, the responses of the various disturbances are evaluated qualitatively and quantitatively. By combining other components analysis, these results may provide the data of the characteristic analysis of the total system and design of control systems.

2. Analysis Model

The evaporator considered was the air cooling type plate fin coil. In the dynamic analysis, it was assumed that the refrigerant flows tube inside and the heating air flows tube outside. Figure 1 shows the temperature distribution model of the refrigerant and the tube wall. The dynamic characteristics were performed with this model. In this figure, each region is divided into a two-phase region, completed evaporation region, and superheated vapor region.

2.1 Assumptions for the model

The mathematical model is based on the following assumptions:

- The inflow air velocity and temperature are uniform.
- The heat transfer coefficient of the outside

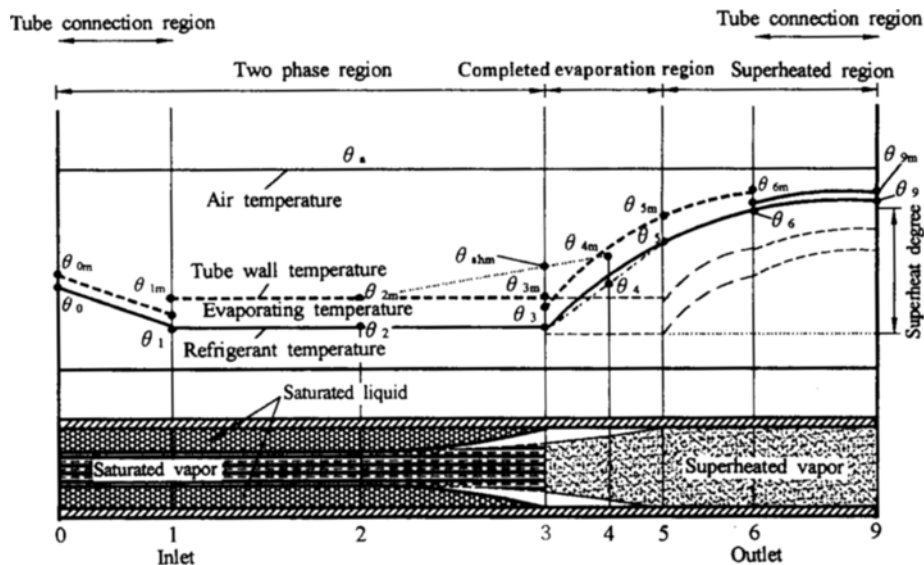


Fig. 1 Model of the refrigerant and tube wall temperature distribution

tube wall changes discontinuously in the two-phase and superheated vapor region, and it is assumed that the fluid velocity does not affect convection heat transfer.

(c) The two-phase refrigerant has linear quality distribution from the inlet to the completed evaporation point, and the refrigerant is assumed to be in a saturated state.

(d) The refrigerant temperature in the two phase region is uniform; the saturation temperature at the completed evaporation point replaces the evaporation pressure.

(f) The pressure drop inside the tube is proportional to the temperature.

(g) The pressure drop is ignored in the superheated vapor region because the length is short, compared with the two-phase region.

2.2 Basic equations

The basic equations of the dynamic characteristics are derived from the continuity, energy equilibrium, and heat transfer equations with above assumptions and analysis model. The two-phase evaporating region is shown in Fig. 1 as a control volume between boundaries 1 and 3. Here, the continuity equation, energy equilibrium equations of the refrigerant and tube wall can be written as:

$$M_1 - M_3 = A \left[\frac{d}{dt} (\bar{\rho}_2 L_{13}) - \rho_3 \frac{dL_{13}}{dt} \right] \quad (1)$$

$$M_1 H_1 - M_3 H_3 + Q_{13} = A \left[\frac{d}{dt} (\bar{\rho}_2 H_2 L_{13}) - \rho_3 H_3 \frac{dL_{13}}{dt} \right] \quad (2)$$

$$\alpha_{2g} A_o^* L_{13} (\Theta_{2g} - \Theta_{2m}) - \alpha_2 A_i^* L_{13} (\Theta_{2m} - \Theta_2) = C_m L_{13} \frac{d\Theta_{2m}}{dt} \quad (3)$$

where $Q_{13} = \alpha_{2g} A_o^* L_{13} (\Theta_{2g} - \Theta_{2m}) + C_m (\Theta_{shm} - \Theta_{2m}) \frac{dL_{13}}{dt} - C_m L_{13} \frac{d\Theta_{2m}}{dt}$

The control volume of the completed evaporation region is shown in boundaries 3 to 5, where the basic equations can be written as:

$$M_3 - M_5 = A \left[\frac{d}{dt} (\rho_4 L_{35}) - \rho_3 \frac{dL_{35}}{dt} \right] \quad (4)$$

$$M_3 H_3 - M_5 H_5 + Q_{35} = A \left[\frac{d}{dt} (\rho_4 H_4 L_{35}) - \rho_3 H_3 \frac{dL_{35}}{dt} \right] \quad (5)$$

$$C_m L_{35} \frac{d\Theta_{4m}}{dt} = \alpha_{sg} A_o^* L_{35} (\Theta_{sg} - \Theta_{4m}) - \alpha_s A_i^* L_{35} (\Theta_{4m} - \Theta_4) \quad (6)$$

where $Q_{35} = \alpha_{sg} A_o^* L_{35} (\Theta_{sg} - \Theta_{4m})$

$$- C_m (\Theta_{4m} - \Theta_{shm}) \frac{dL_{35}}{dt} - C_m L_{35} \frac{d\Theta_{4m}}{dt}$$

The control volume in the superheated region is shown in boundaries 5 to 6, where the basic equations can be written as:

$$M_5 = M_6 \quad (7)$$

$$M_5 C_p \frac{\partial \Theta}{\partial l} + A \rho_{56} c_p L_{56} \frac{\partial \Theta}{\partial t} = \alpha_s A_i^* L_{56} (\Theta_m - \Theta) \quad (8)$$

$$C_m L_{56} \frac{\partial \Theta_m}{\partial t} = \alpha_{sg} A_o^* L_{56} (\Theta_{sg} - \Theta_m) - \alpha_s A_i^* L_{56} (\Theta_m - \Theta) \quad (9)$$

where, L_{56} is the length from boundary 5 to any position in this region, $l = (L_{56}/L_{560})$ is the dimensionless position in boundary 5, and Θ is the refrigerant temperature of the superheated vapor in the dimensionless position (i), and Θ_m is the tube wall temperature.

2.3 Combination and linearization of basic equations

By combining basic equations in each region, each change in quantity describes the sums of the equilibrium state quantity and perturbation quantity, i. e., where the operation of the evaporator is considered from the equilibrium state to perturbation, which is linearized, and infinitesimal items of higher degree are ignored. When the inlet refrigerant flow rate changes, in the two-phase evaporating region, the linearized energy equilibrium equation of the refrigerant can be written as:

$$M_{10} (H_{30} - H_{10}) = \alpha_2 A_i^* L_{130} (\Theta_{2m0} - \Theta_{20}) \quad (10)$$

$$(H_{30} - H_{10}) m_1 = \alpha_2 A_i^* (\Theta_{2m0} - \Theta_{20}) l_{13} + \alpha_2 A_i^* L_{130} (\Theta_{2m} - \Theta_2) + [A (\bar{\rho}_{20} H_{30} - \bar{\rho}_{20} H_{20}) + C_m (\Theta_{shm0} - \Theta_{2m0})] \frac{dL_{13}}{dt} \quad (11)$$

Using the same method, the linearized energy equilibrium equation of tube wall can be written as:

$$\alpha_{2g} A_o^* (\Theta_{2g0} - \Theta_{2m0}) = \alpha_2 A_i^* (\Theta_{2m0} - \Theta_{20}) \quad (12)$$

$$C_m \frac{d\theta_{2m}}{dt} = \alpha_2 A_i^* \theta_2 - (\alpha_2 A_i^* + \alpha_{2g} A_o^*) \theta_{2m} \quad (13)$$

The linearized energy equilibrium equation of the refrigerant in the completed evaporation region is given by:

$$\begin{aligned} (H_{50} - H_{30})m_1 &= \alpha_s A_i^* L_{350} (\theta_{4m} - \theta_4) \\ &\quad - M_{10} C_p \theta_5 \frac{d\theta_5}{dt} - A \rho_{40} L_{350} \frac{C_p}{2} \\ &\quad - \alpha_3 A_i (\Theta_{4m0} - \Theta_{40}) l_{13} \\ &\quad + \{A[\rho_{40}(H_{40} - H_{50}) \\ &\quad + \bar{\rho}_{20}(H_{50} - H_{30})] \\ &\quad + C_m (\Theta_{4m0} - \Theta_{sh0})\} \frac{dl_{13}}{dt} \end{aligned} \quad (14)$$

Using the same method, the linearized energy equilibrium equation of the tube wall can be written as:

$$C_m \frac{d\theta_{4m}}{dt} = \alpha_s A_i^* \theta_4 - (\alpha_s A_i^* + \alpha_{sg} A_o^*) \theta_{4m} \quad (15)$$

The energy equilibrium equations of the refrigerant and tube wall in the superheated vapor region can be written as:

$$M_{10} C_p \frac{\partial \Theta}{\partial l} + A \rho_{560} C_p L_{560} \frac{\partial \Theta}{\partial t} = \alpha_s A_i^* L_{560} (\Theta_m - \Theta) \quad (16)$$

$$C_m \frac{\partial \Theta_m}{\partial l} = \alpha_{sg} A_o^* (\Theta_{sg} - \Theta_m) - \alpha_s A_i^* (\Theta_m - \Theta) \quad (17)$$

Also, in each region, derivation of the linearized equations along with each disturbance such as inlet refrigerant enthalpy change, air temperature and air velocity is possible by the same method on the inlet refrigerant flow rate change.

2.4 Transfer functions and block diagram

The transfer functions of the dynamic characteristics analysis are obtained by the Laplace transformation of the linearized heat energy equilibrium equations. When the refrigerant flow rate changes, in the two-phase evaporating region, the transfer function is represented as:

$$\begin{aligned} m_1(s) e^{-\tau_{130}s} + \frac{1}{K_{2A}} \left\{ 1 - \frac{K_{2B}}{(1 + T_{2A}s)} \right\} \theta_2(s) \\ = \frac{(1 + T_2s)}{K_2} l_{13}(s) \end{aligned} \quad (18)$$

The transfer function of the completed evaporation region can be written as:

$$\begin{aligned} \frac{K_4}{(1 - T_4s)} e^{-\tau_{130}s} m_1(s) \\ + \frac{K_4}{K_{4A}(1 - T_4s)} \left\{ 1 - \frac{K_{4B}}{(1 + T_{4A}s)} \right\} \theta_3(s) \\ + \frac{K_4}{K_{4A}(1 - T_4s)} \left\{ 1 - \frac{K_{4B}}{(1 + T_{4A}s)} \right\} \theta_5(s) + l_{13}(s) \\ = - \frac{K_4(1 + T_{4B}s)}{K_{4C}(1 - T_4s)} \theta_5(s) \end{aligned} \quad (19)$$

The transfer function of the superheated vapor region is represented as:

$$\frac{\theta_6(s)}{\theta_5(s)} = e^{-f(s)} = e^{-[\alpha + \tau_a s + C \frac{\tau_w s}{(1 + \tau_w s)}]} \quad (20)$$

where, $e^{-\alpha}$ is the gain constant of the static characteristic, τ_a is the time delay constant by the transportation delay, and $C\tau_w s/(1 + \tau_w s)$ is the phase delay parameter, which is the effect of heat capacity in the tube wall. Also, in each region, the transfer functions of the dynamic characteristics analysis along each disturbance such as inlet refrigerant enthalpy change, air temperature and air velocity are obtained by the same method for the inlet refrigerant flow rate change. The block diagrams of each region were drawn through the transfer functions of the region, and the whole block diagram under the various disturbances can be described by the combination of transfer functions of each region such as the two-phase, the saturated vapor and the superheated vapor region.

3. Results and Discussion

3.1 Responses of each region

The response characteristics were analyzed from the Bode diagram in the frequency response

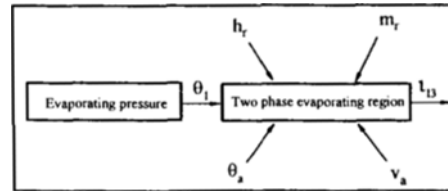


Fig. 2 Block diagram of the two-phase evaporating region

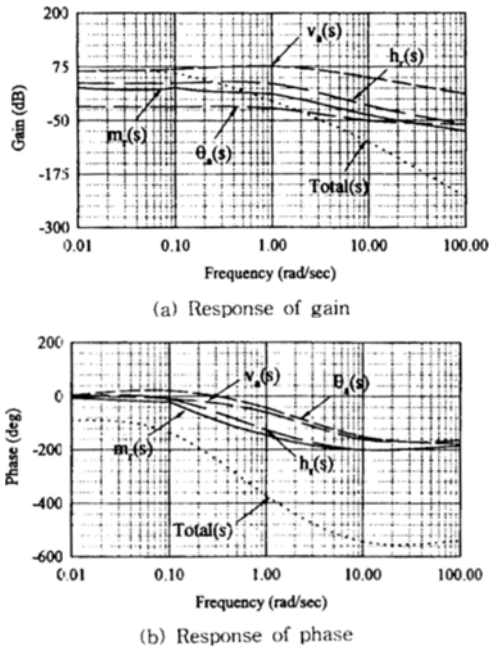


Fig. 3 Responses of length in the two-phase evaporating region

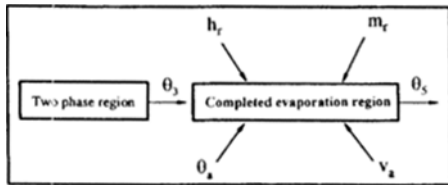


Fig. 4 Block diagram of the completed evaporation region

method. It was performed separately under each disturbance and combined disturbances. Figure 2 shows the block diagram of the two-phase evaporating region, and Fig. 3 shows the responses of length of this region in the frequency response method when various disturbances were input parameters. In the gain diagram of Fig. 3(a), the change of inflow air velocity showed large gain response in the total frequency range. Also, substantially each disturbance showed high gain value in the low frequency band, but these showed decreasing tendency when moving toward the high frequency band. It is believed to be that the heat transfer coefficient of

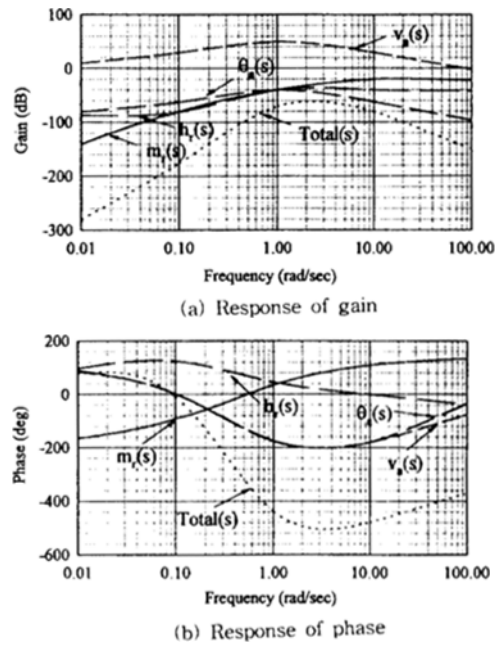


Fig. 5 Responses of outlet temperature in the completed evaporation region

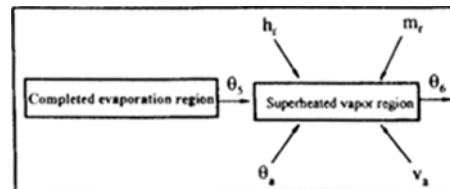


Fig. 6 Block diagram of the superheated vapor region

the refrigerant side and evaporating temperature affect largely in this region. In the phase diagram of Fig. 3(b), the change of inflow air temperature showed the lowest phase delay, the change of the refrigerant flow rate showed the highest. The reason is that the change of flow rate accompanies the time delay, thus the time delay constant affects the phase delay. The total phase response showed the response characteristics of higher degree.

As the same method, Fig. 4 shows the block diagram of completed evaporation region, and Fig. 5 shows the responses of outlet temperature in this region. In the gain diagram of Fig. 5(a), the change of inflow air velocity showed the

largest response, and the change of refrigerant flow rate showed increasing tendency when moving toward the high frequency range. The gain response of total disturbances showed the highest in a frequency of 5×10^0 . In the phase diagram of Fig. 5(b), the change of inflow air temperature

and velocity showed almost similar tendency; the change of refrigerant flow rate showed small phase delay when moving toward the high frequency band. It is believed to be that the refrigerant in this region is in a saturated state, so the heat capacity of the tube wall affects the gain and time delay constants which affect the responses of length.

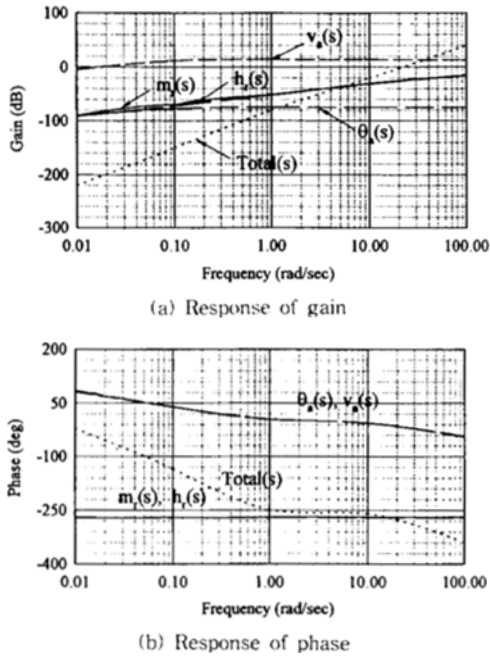


Fig. 7 Responses of the outlet temperature in the superheated vapor region

Figure 6 shows the block diagram of the superheated vapor region, and Fig. 7 shows responses of the outlet temperature in this region. In the gain diagram of Fig. 7(a), each disturbance showed almost no influence on the total frequency range, and when the various disturbances input simultaneously, the response increased when moving toward the high frequency band. In the phase diagram of Fig. 7(b), the change of the refrigerant flow rate and inlet enthalpy, and the change of the inflow air temperature and velocity showed similar tendency, respectively. And the total phase delay showed an item of higher degree. It is believed to be that the refrigerant in this region is in a superheated vapor state and the heat transfer coefficients on the refrigerant and tube wall side and temperatures of refrigerant and tube wall almost were not affected from the various disturbances.

3.2 Responses of total region

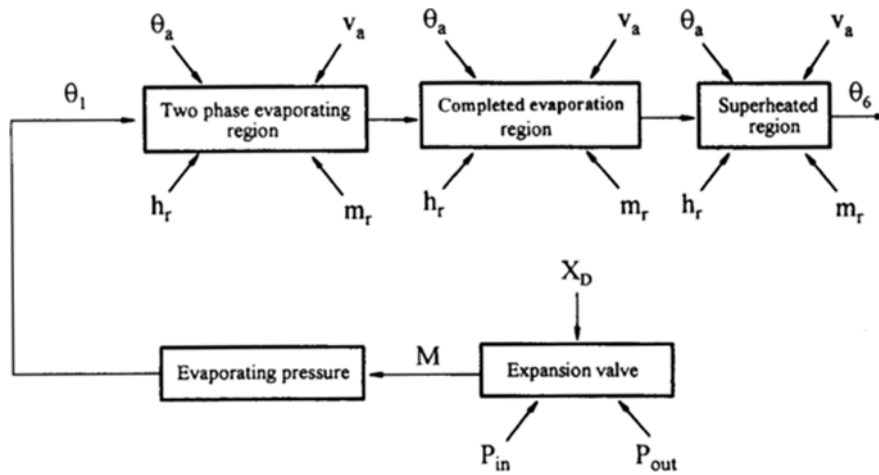


Fig. 8 Block diagram of the evaporator

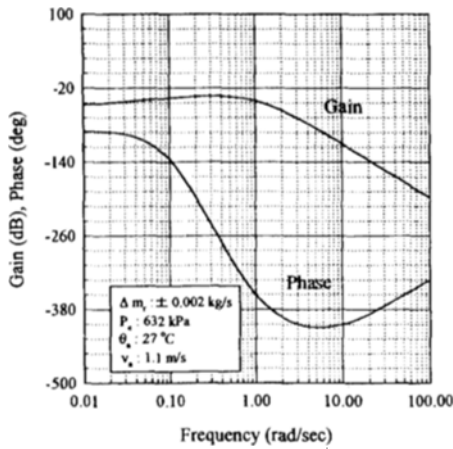


Fig. 9 Response of the evaporator outlet temperature (θ_6) depend on the change of refrigerant flow rate

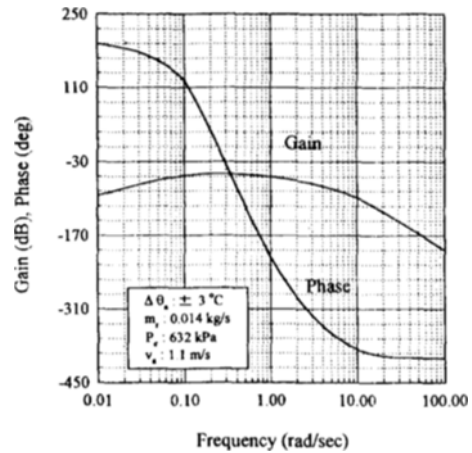


Fig. 11 Response of the evaporator outlet temperature (θ_6) depend on the change of air temperature

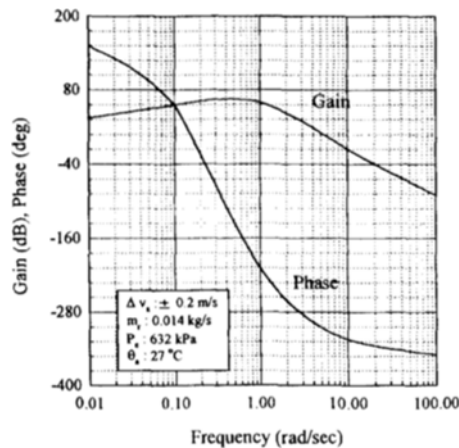


Fig. 10 Response of the evaporator outlet temperature (θ_6) depend on the change of air velocity

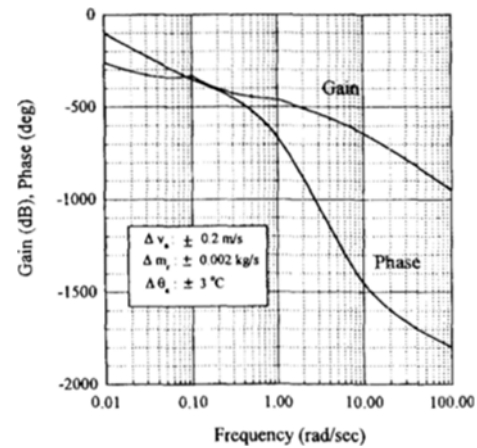


Fig. 12 Response of the evaporator outlet temperature (θ_6) in the evaporator

From the results of the dynamic characteristics in each region, the dynamic response of the outlet temperature in the evaporator was analyzed by combining the transfer functions of each region in the block diagram when various disturbances were operating in the evaporator. Figure 8 shows the block diagram of the total evaporator as well as the transfer functions of each region in the evaporator.

Figure 9 shows the response of the outlet temperature (θ_6) in the evaporator when the change of the refrigerant flow rate is operating in the

total region of the evaporator. In this figure, the results showed a higher tendency in the low frequency band, which decreased when moving toward the high frequency band. These results showed differences from that of Fig. 7 only in the superheated region. The reason is that the time delay and time constants were affected by the heat capacity of the tube wall, the heat transfer coefficients on the refrigerant and tube wall side.

Figure 10 shows the response of the outlet temperature (θ_6) in the evaporator when the change of air velocity is operating in the total

region of the evaporator simultaneously. Figure 11 shows the evaporator outlet temperature (θ_6) when the change of air temperature is operating in the total region of the evaporator simultaneously. In these figures, the gain and phase values showed almost similar tendency qualitatively with that of Fig. 9, but they differed quantitatively in the whole frequency range. Gain, time constant and time delay were considered on the basis of the heat transfer coefficient on the refrigerant and air side.

Figure 12 shows the response of the outlet temperature (θ_6) in the total evaporator when the disturbances, such as change of refrigerant flow rate, air velocity, and air temperature, are operating simultaneously. In this figure, the responses of gain and phase showed different trends in each disturbance input, respectively.

4. Conclusions

The transfer functions of the dynamic characteristics in the evaporator were obtained from the basic equations, linearizations and Laplace transformations of equations for the various kinds of disturbance input. The analyses of the dynamic characteristics were performed by the frequency response method, and results of this study can be described as follows:

The development of a block diagram on the dynamic characteristics analysis in the evaporator become possible by linearizations of the basic equations, derivation of transfer functions, and combination of these with various kinds of disturbance input. Effects of various disturbances on the actual evaporators were analyzed by the frequency response method, and the basic design data in the evaporator were obtained quantitatively and qualitatively. Sufficient data were obtained to analyze the dynamic characteristics in the total system on the basis of these results. Therefore, these results may be used to evaluate hardware and optimal design parameters, design control systems and determine the best controller settings

for the refrigeration and air conditioning systems.

References

- Higuchi, K., 1986, "Electronic Expansion Valve and Control," *Japanese Association of Refrigeration*, Vol. 61, No. 701, pp. 1~8.
- Higuchi, K., 1987, "Dynamic Simulations of a Vapor Compression Type Heat Pump (Frequency Response and Stability of a System)," *Japanese Association of Refrigeration Heat Pump Report*, pp. 87~104.
- Hiroumu, I., 1985, "Automatic Control Machinery of Refrigeration," *Japanese Association of Refrigeration*, pp.1~157.
- Honma, I., 1992, "Design of Refrigerant Flow Rate Control System by Electric Expansion Valve," *Proceedings of 1992 JAR Annual Conference*, pp. 105~108.
- Kim, J. D., Oh, H. K. and Yoon, J. I., 1994, "A Study on Dynamic Characteristics of Refrigeration System by Controlling of the Evaporator Superheat", *Proceedings of 1994 Korean Journal of Air-Conditioning and Refrigeration Engineering*, pp. 207~211.
- Kim, J. D., Oh, H. K. and Yoon, J. I., 1996, "A Study on Optimal Control of Multi-Air Conditioning System," *Proceedings of the KSME 1996 Spring Annual Meeting A*, pp. 276~282.
- Matsuoka, A., 1988, "Electronic Control of Air-Conditioner," *Japanese Refrigeration and Air-Conditioning Industry Association*, pp. 3~72.
- Tanaka, N. and Yumikura, T., 1980, "Holding Amount of Refrigerant in Air Conditioners and its Dynamic Properties," *Japanese Association of Refrigeration*, Vol. 55, No. 633, pp. 5~13.
- Wang, H. and Touber, S., 1991, "Distributed and Non-Steady-State Modelling of an Air cooler," *International Journal of Refrigeration*, Vol. 14, pp. 98~111.
- Yasuda, H., Ishibane, K. and Nakayama, S., 1992, "Evaporator Superheat Control by An Electrically Driven Expansion Valve," *Trans. of the JAR*, Vol. 9, No. 2, pp. 147~156.